Engineering 56 (2026) 306–316

Contents lists available at ScienceDirect

Engineering

journal homepage: www.elsevier.com/locate/eng

Research
Climate Change—Article

Nature-Based Global Land Surface Soil Organic Carbon Indicates Increasing Driven by Climate Change

Yanli Liu [a,b,c,#,*], Xin Chen [a,d,#], Jianyun Zhang [a,b,c,*], Xing Yuan [e], Tiesheng Guan [a,b,c], Junliang Jin [a,b,c], Guoqing Wang [a,b,c]

[a] The National Key Laboratory of Water Disaster Prevention, Nanjing Hydraulic Research Institute, Nanjing 210029, China
[b] Yangtze Institute for Conservation and Development, Nanjing 210098, China
[c] Research Center for Climate Change of Ministry of Water Resources, Nanjing 210029, China
[d] State Key Laboratory of Simulation and Regulation of Water Cycle in River Basin, China Institute of Water Resources and Hydropower Research, Beijing 100038, China
[e] School of Hydrology and Water Resources, Nanjing University of Information Science and Technology, Nanjing 210044, China

ARTICLE INFO

Article history:
Received 20 February 2024
Revised 10 September 2024
Accepted 31 March 2025
Available online 12 April 2025

Keywords:
Soil organic carbon
Climate change
Carbon sink
Paris Agreement plan

ABSTRACT

Soil could represent a potentially notable source of carbon for achieving global carbon neutrality. However, how the land surface soil organic carbon (SOC) stock, which is more sensitive to climate change than other carbon stocks, will change naturally under the influence of global warming remains unknown. In this work, the global land surface SOC trends from 1981 to 2019 were explored, and the driving factors were identified. A random forest model (a type of machine learning method) was proposed to predict future global surface SOC trends integrated with climate scenarios of the Coupled Model Intercomparison Project Phase 6 (CMIP6) models. The results revealed that the global surface SOC content will increase, while the temperature and precipitation are the main climate drivers at the global scale, and vegetation cover is a crucial local factor influencing the increase in SOC. However, under the 1.5 °C global warming scenario, the land SOC sink will increase by 13.0 petagram carbon (PgC) at most compared with that under the SSP2-4.5 scenario, which accounts for only 19% of the total carbon emission capacity at the current 1.1 to 1.5 °C global warming level. Moreover, this value is far from the Paris Agreement target of four out of one thousand for the annual increase in the soil carbon stock 40 cm below the surface over the next 20 years (2.72 PgC·a^{-1}). This illustrates that overreliance on natural carbon sinks is a high-risk strategy. These findings highlight the urgency of implementing mitigation and removal strategies to reduce greenhouse gas emissions.

© 2025 THE AUTHORS. Published by Elsevier LTD on behalf of Chinese Academy of Engineering and Higher Education Press Limited Company. This is an open access article under the CC BY-NC-ND license (http://creativecommons.org/licenses/by-nc-nd/4.0/).

1. Introduction

Soil is one of the main carbon stocks in land surface systems. The soil organic carbon (SOC) stock is approximately 1.5 trillion tonnes, storing approximately twice the amount of carbon in the atmosphere and approximately three times that in terrestrial vegetation [1]. Specifically, the land surface SOC stock at 30 cm below the surface is approximately 0.68 trillion tonnes, which is also much greater than that in the atmosphere and vegetation. Even a slight variation in the SOC stock could greatly influence the atmospheric carbon dioxide (CO_2) concentration and play an essential role in regulating the carbon neutrality of global terrestrial ecosystems. Among the targets of the 2015 Paris Agreement, the "4 per 1000" Initiative was proposed, which aimed to achieve a four out of one thousand increase per year in the soil carbon stock 40 cm below the surface over the next 20 years, with the potential to significantly reduce the carbon budget for climate stabilization under the 2 °C global warming scenario [2,3]. However, changes in soil carbon exhibit a particularly high uncertainty [4–7], and models differ regarding the direction of the change in carbon stocks over the past 60 years [8]. The response of SOC at the global scale to greenhouse warming remains unknown. To project the carbon cycle in the future and propose corresponding measures, there is an urgent need to better understand the variation in SOC and its underlying drivers under changing climate conditions.

Studies [9,10] have shown that the SOC content mainly depends on surface vegetation and the land use type and is significantly correlated with residual plant leaves entering the soil and with soil

* Corresponding authors.
E-mail addresses: ylliu@nhri.cn (Y. Liu), jyzhang@nhri.cn (J. Zhang).
# These authors contributed equally to this work.

https://doi.org/10.1016/j.eng.2025.03.031
2095-8099/© 2025 THE AUTHORS. Published by Elsevier LTD on behalf of Chinese Academy of Engineering and Higher Education Press Limited Company.
This is an open access article under the CC BY-NC-ND license (http://creativecommons.org/licenses/by-nc-nd/4.0/).

microbial species. Owing to the intricacy of climate–plant–soil interactions, the carbon cycle is complex due to the influence of climate factors, the spatial and temporal variability in vegetation cover conditions, and the biological and soil controls on plant growth and organic matter decomposition [11]. Over the last 60 years, there has been a continuous increase in anthropogenic CO_2 emissions [8], which has resulted in global warming. Climate change controls SOC dynamics in terms of temperature and precipitation [12] and is the most important driver of SOC stocks [13]. These control factors can potentially accelerate or decelerate future SOC stocks and affect atmospheric greenhouse gas concentrations. In the 21st century, there has been an overall increase in global SOC stocks, as projected by process-based vegetation models [14,15]. Climate change and variations in the atmospheric CO_2 concentration fulfill important roles in modulating terrestrial carbon sinks [16,17] and induce changes in the vegetation structure (i.e., the leaf area index (LAI)), which in turn causes changes in the carbon cycle. Although the increase in the LAI in recent decades has been significant, the feedback of the LAI to the carbon cycle has not been studied systematically [18], nor has the SOC content, which greatly affects the structure and properties of soils, thus influencing vegetation productivity. Under a future warming climate, whether soils serve as carbon sinks or sources depends on plant growth and soil decomposition.

Understanding the effects of climate change on global SOC levels is critical for assessing the potential for future climate change mitigation through SOC management or land use decisions. Owing to the insufficient understanding of the global SOC mechanism and the high uncertainty in models, the future SOC variation remains uncertain even with the occurrence of both negative and positive feedback. Many studies have focused on the microscopic mechanism of microbial decomposition, biological carbon, and sequestration effects [19–22], which are mainly based on the steady-state assumption of SOC at regional scales. However, the steady-state assumption does not hold at the global scale. Machine learning methods provide another solution for exploring the dynamic variations in the global SOC concentration, thereby fully utilizing their data mining advantage in identifying inherent correlations and mechanisms from long time series on large scales. Nevertheless, future climate scenarios are essential for SOC projections. In previous studies, different global climate models (GCMs) have been used to study the impacts of climate change on SOC stocks in different countries [23,24]. There are considerable variations in future climate projections, especially in terms of seasonal rainfall, among different GCMs [25], but a multi-GCM ensemble under different emission scenarios can provide a more robust assessment of the impacts of climate change [26,27]. Compared with the Coupled Model Intercomparison Project Phase 5 (CMIP5) projections, CMIP6 projections indicate that the annual mean temperature will continue to increase, resulting in a higher probability of meteorological drought [28]. CMIP6 projections are considered less biased simulations [29], and knowledge of how future climate change might affect SOC stocks is crucial for developing management strategies to minimize SOC decline [30]. Current studies [31–34] have focused mainly on the SOC variation status on a regional scale, such as a certain country or a type of land cover, whereas few studies have focused on global SOC variations, especially via new CMIP6 climate scenarios. It is crucial to explore the dynamic variations in SOC at the global scale for effective management and decision-making purposes and to predict the fate of the largest terrestrial carbon stock [35]. Nature-based variations in SOC effectively influence human-driven actions to achieve the objective of a soil sink. However, how the land surface SOC stock, which is more sensitive to climate change than other carbon stocks, will change naturally under the influence of global warming remains unknown.

Thus, the goal of this study was to analyze the mechanism by which climate factors influence natural global land surface SOC stocks and predict future trends under continued global warming. A random forest (RF) model was proposed that integrates the inherent mechanism, as deduced from large-scale long time-series data. This paper is organized as follows. In Section 2, the data and methods for SOC trend analysis, driving factor identification, simulation, and projection are provided. Next, the historical characteristics of the global land surface SOC concentration from 1981 to 2019 are explored in Section 3.1, and the drivers are identified in Section 3.2. The accumulation and migration routes of global SOC storage are revealed in Section 3.3. An RF model is proposed and calibrated via a historical series, which is employed to predict future change trends (Section 3.4). To validate the model results, a comparison analysis is conducted in Section 4. Finally, conclusions are provided in Section 5. The findings of this study could provide a greater understanding of the evolution mechanism of global surface SOC levels and the role of potential natural carbon sinks driven by climate change.

2. Materials and method

2.1. Data

TerraClimate data are incorporated into global observed climate data, including temperature, precipitation, evaporation, wind, and runoff data. The LAI product employed in this paper is the global 5 km 8 day LAI product. The SOC product is derived from the global 1 km surface SOC pool (SOC-1 km) dataset released by the National Science and Technology Infrastructure of China. This product includes surface layer (0–30 cm) SOC pool (tonne of carbon per hectare ($tC{\cdot}ha^{-1}$)) data from 1981 to 2019 with a 1 km resolution. The temporal resolution is one year and includes a coordinate reference system, time range, spatial range, and SOC density information [36,37]. This dataset comprises gridded high-resolution and long time-series data and can be used for examining the inherent evolution mechanism. Owing to the current considerable uncertainty in global surface SOC calculations, to demonstrate the feasibility of this dataset, three global SOC stock datasets, namely, World Soil Information Service (WoSIS), SoilGrids and Harmonized World Soil Database (HWSD), were employed for comparison (Text S1 in Appendix A).

Projections under future climate scenarios (namely, shared socioeconomic pathways SSP1-2.6, SSP2-4.5, SSP3-7.0, and SSP5-8.5), as generated by 11 GCMs (Table S1 in Appendix A), were obtained from the CMIP6.

2.2. Analysis of the global SOC trends

To explore the change trends of historical global SOC levels, the Theil–Sen median trend method was employed, which was combined with the Mann–Kendall test method. The general trend in the SOC data series was first objectively analyzed via the Theil–Sen median trend method and the significance of the obtained SOC variation trend was assessed via the Mann-Kendall test method (Table S2 in Appendix A).

2.3. Analysis of the driving factors

We applied the geographical detector model to analyze the driving factors of global SOC change. The geographical detector model can be used to effectively analyze the relative importance of different influencing factors to the target, thereby preventing human subjectivity from interfering with the selection and

calculation of evaluation factors. This model comprises four modules: risk, factor, ecological, and interaction detection modules.

The factors of temperature, precipitation, and vegetation have generally been chosen for SOC analysis [38,39], and the synergistic effect of climate factors and vegetation impacts SOC [40,41]. Moreover, environmental factors such as rainfall frequency, wind speed, and runoff affect the retention time of SOC to different degrees [42–44]. Thus, based on the analysis of the formation conditions and dynamics of SOC changes, we selected precipitation, temperature, evaporation, wind speed, rainfall days, average runoff depth, and LAI as potential factors. By using the geographical detector model (Text S2 in Appendix A), we quantitatively analyzed the impacts of various factors and their interactions on global SOC storage via the factor and interaction detection modules and revealed the driving mechanism of SOC spatial differentiation in different regions. The driving force size interval and the type of interaction are provided in Table S3 in Appendix A.

2.4. Historical SOC simulation and future projection

We applied the RF model to simulate the historical global SOC levels and project future variations. Based on the integration of decision trees, this model is a classifier in which multiple decision trees are employed for training to predict samples. As a robust and accurate machine learning method, it provides the advantages of low susceptibility to overfitting and aims to evaluate the relative importance of each feature. Even if data are partially missing, accuracy could still be guaranteed. In this study, we adopted precipitation, temperature, evaporation, wind speed, rainfall days, average runoff depth, and LAI as potential factors to predict global and continental annual average SOC concentrations. Sample datasets of historical factors and SOC levels from 1981 to 2019 were obtained. The model was trained and validated via annual data from 1981 to 2019, and a spatial resolution of $0.5^\circ \times 0.5^\circ$ was chosen to ensure spatial matching between the various input data.

The main steps of the algorithm are as follows: ① K distinct sample datasets are extracted from the original dataset via the bootstrap method, which is employed as subtraining sets for each decision tree. The sample size is the same as that of the original dataset. ② Each sample training set is used to generate the corresponding K sample datasets, which are used as subtraining sets for each decision tree, and the sample size is the same as that of the original dataset. ③ For the test data, each decision tree is separately employed for testing to obtain the prediction value of the corresponding decision tree. ④ The forecast results of the K decision trees are averaged to obtain the final forecast result.

The model parameter of the maximum depth of the tree was adjusted via the grid search method in Python. We set the maximum depth to 55 to achieve high prediction accuracy in the experiments. We set the number of trees to 500. The R-squared values for different years at the global and continental scales were calculated to evaluate the model performance. The simulation performance of the RF model is shown in Fig. S1 in Appendix A. The results revealed that the minimum R-squared value is 0.67 for Europe, and the remaining continental-scale R-squared values are above 0.84, which indicates very good performance, and the model could be applied to predict future SOC levels.

Thus, with the use of the validated RF model, we predicted the future global SOC concentration on a yearly basis based on CMIP6 scenarios of 11 GCM models under four shared socioeconomic pathways, namely, SSP1-2.6, SSP2-4.5, SSP3-7.0, and SSP5-8.5, using the precipitation, temperature, evaporation, wind speed, rainfall days, average runoff depth, and LAI as inputs. Any missing data under some scenarios were replaced with GCM-averaged values.

3. Results

3.1. Historical characteristics of the global land surface SOC stock from 1981 to 2019

The global and continental SOC contents generally increased after 1990, although a slight decline or a brief fluctuation period occurred from 1981 to 1990 (Fig. 1). The global climate and underlying surface conditions have greatly changed since the 1990s, which has exerted more diversified and accelerated impacts on SOC. In North America, Europe, and Asia, the trend change around 1990 was quite significant. In South America and Africa, where the vegetation cover is relatively high (Fig. S2 in Appendix A), the SOC increased continuously.

Overall, the global SOC stock was concentrated in high- and mid-latitude regions in the Northern Hemisphere, accounting for 73% of the global land surface SOC storage (Fig. S2). Except for high-latitude regions, the SOC stock is closely related to vegetation cover and generally consistent with the spatial distribution of the LAI (Fig. S2). Notably, the opposite trends involve a decrease in North Asia and an increase in South Africa and North America (Fig. S3 in Appendix A). Thus, we explored the anomalous variations in SOC storage at different latitudes across each continent, as shown in Fig. 2. Notably, the mid- and high-latitude SOC reserves in most regions of the world first decreased and then slowly increased, whereas the SOC reserves in low-latitude regions basically exhibited a continuous increase, as detailed in Table 1. This phenomenon could be attributed to the increase in vegetation cover at low latitudes (Fig. S2) and soil decomposition at high latitudes induced by global warming over the past 40 years.

In general, the global SOC stock increased by 6.393 PgC from 1981 to 2019 (Table 1). Notably, in high-latitude and high-altitude regions with large carbon stocks, such as Asia, North America, and Europe, SOC showed a remarkable decrease of 1.266 PgC. These findings suggest the high potential for SOC release in the future under the influence of warming. In contrast, SOC increased by 7.658 PgC in the mid- and low-latitude regions of all continents except North America. The increases were significant in regions with high vegetation coverage and agricultural planting (Fig. S4 in Appendix A), and vegetation plays a key role in the SOC reserves derived from photosynthesis and respiration (Fig. S5 in Appendix A).

From 1981 to 2019, the global average precipitation, temperature, and LAI increased (Fig. S6 in Appendix A). The increase in precipitation and temperature obviously facilitates vegetation growth, which in turn increases the SOC reserves. In frozen soil zones, an increase in the temperature can accelerate the melting process, which results in the release of the original sequestered carbon and, more easily, of the land surface SOC stock. In addition, wind and flow factors influence land surface SOC variation via erosion. Thus, it is necessary to comprehensively explore the drivers and their synergistic effect on global land surface SOC stocks.

3.2. Drivers of the change in global land surface SOC stocks

Climate, water, and land cover conditions can cause changes in SOC. Thus, we selected precipitation, temperature, evaporation, wind speed, rainfall days, average runoff depth, and LAI as potential factors. These factors are not independent and jointly influence SOC changes. The correlation coefficient was calculated via the geographical detector model. The relative importance and interaction factors determined via the RF model and the geographical detector model, respectively, were employed as evaluation indicators to analyze the correlation, importance, and impact of each element on SOC change (Fig. 3). On a global scale, SOC variation

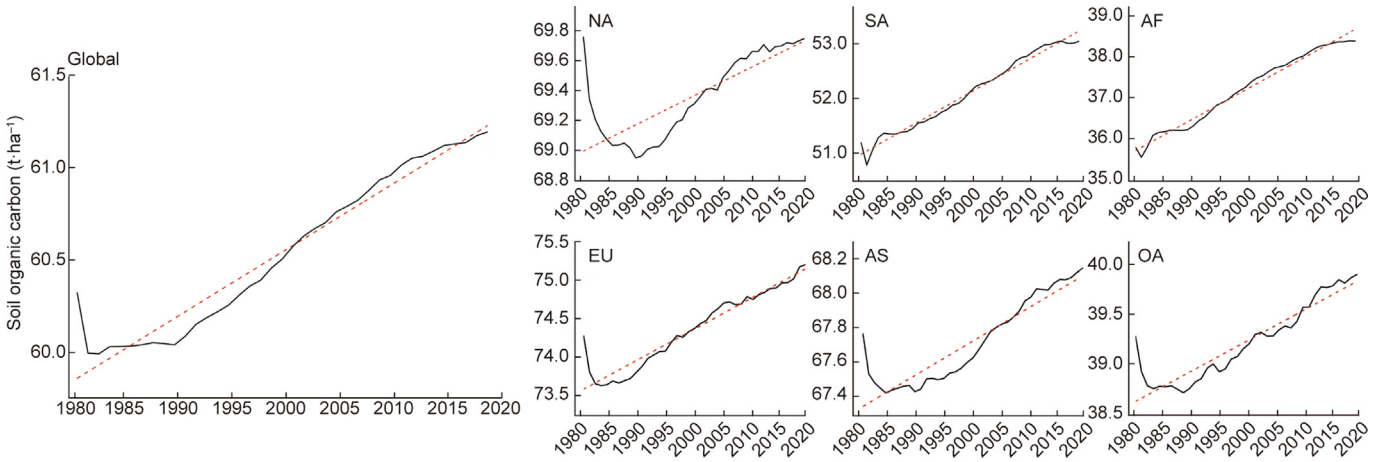

Fig. 1. Changes and trends in the global and continental SOC storage levels from 1981 to 2019. NA: North America; SA: South America; AF: Africa; EU: Europe; AS: Asia; OA: Oceania.

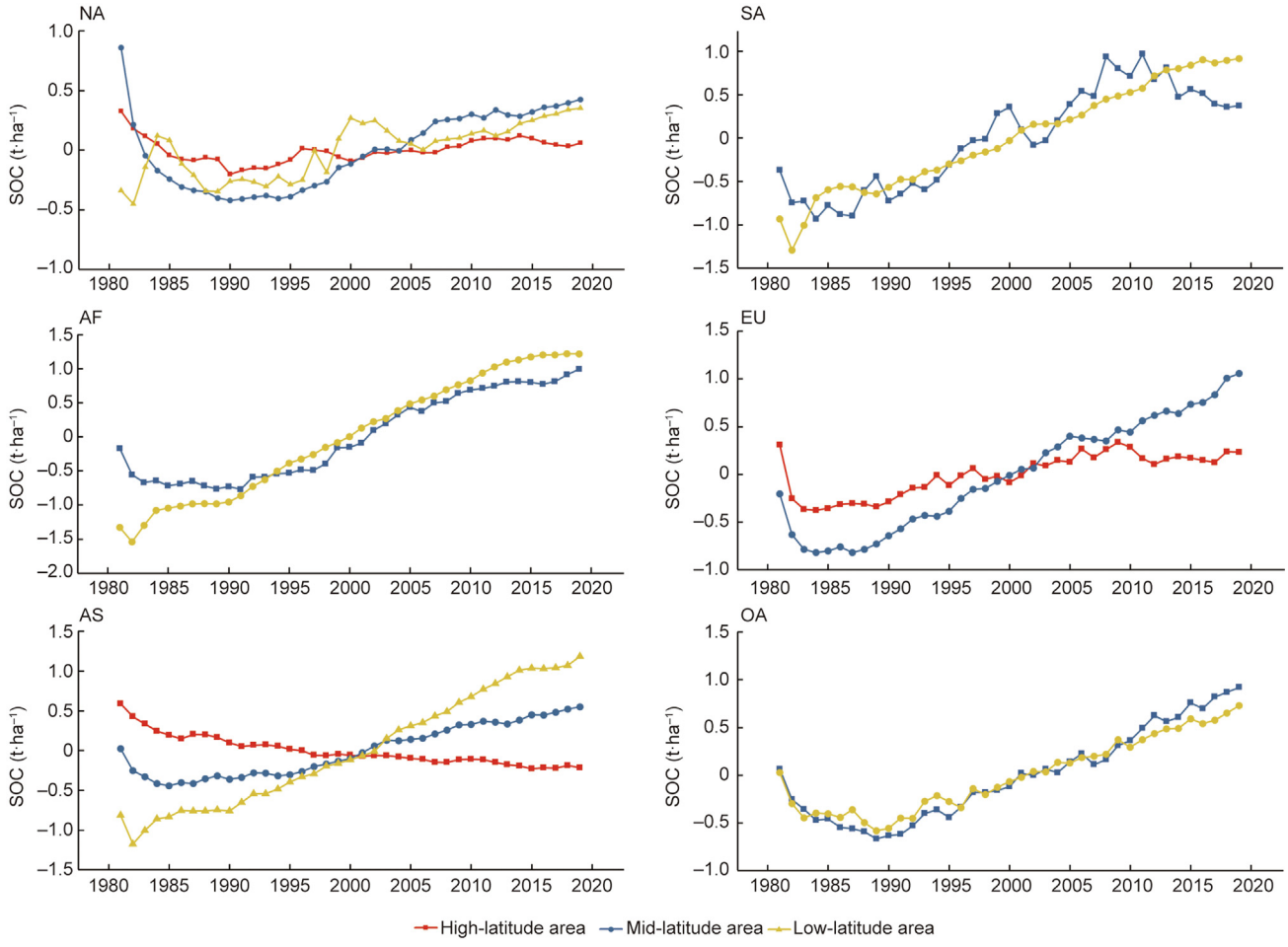

Fig. 2. Anomalous variation in SOC storage at different latitudes across each continent.

is affected mainly by the air temperature, LAI, and rainfall days. The air temperature and LAI positively affect SOC sinks. In contrast, rainfall days yield a negative effect, which is related to potential water erosion of the topsoil layer. The other factors are inconsistent across continents. In addition to the temperature and LAI, the rainfall days plays a key role in determining SOC sinks in North America. Notably, wind speed is one of the key positive drivers of SOC sinks in South America, which differs from that on other continents and could be due to its influence on SOC in Amazon tropical forests. The wind data show high correlation and importance coefficient values in South America, as shown in Fig. 3. Evaporation is very important for SOC changes in Africa. The wind speed and

Table 1
SOC (petagram carbon (PgC)) average (in parentheses) and variation (in bold) across continents from 1981 to 2019.

Continent	NA	SA	AF	EU	AS	OA
High-latitude area (60°–90°)	**−0.233** (69.783)	—	—	**−0.033** (20.115)	**−1.000** (101.278)	—
Mid-latitude area (30°–60°)	**−0.686** (80.387)	**0.129** (12.865)	**0.037** (1.295)	**0.908** (56.719)	**0.768** (119.081)	**0.119** (9.487)
Low-latitude area (0°–30°)	**0.087** (9.799)	**1.557** (51.119)	**3.326** (52.760)	—	**1.115** (30.211)	**0.298** (23.385)
Global	**−0.832** (159.970)	**1.686** (63.984)	**3.364** (54.055)	**0.875** (76.835)	**0.883** (250.571)	**0.417** (32.871)

rainfall days are key negative drivers of SOC sinks in Europe and Asia. The runoff depth yields considerable contributions in Oceania.

Moreover, the interactive effects of factors can cause SOC changes. As shown in Fig. 3, the temperature and LAI are the main factors influencing global SOC stocks and generally yield dual factor increases with other factors across the various continents. Other factor groups exhibit regionally different performance levels across the different continents. In addition to the temperature and LAI, precipitation and evaporation exhibit dual factor increases with other factors in North America, Europe, and Asia. In South America, Africa, and Oceania, the dual factor enhancements decrease, and only the temperature and LAI groups yield similar effects to those of the other factors. The factors with high correlation and importance coefficient values exhibit a high probability of dual factor enhancement with other factors. The impact of a single factor, such as the temperature or LAI, decreases from high to low latitudes, and the interactive effects of factors become more complex. In addition to dual factor enhancement, the factor groups demonstrate nonlinear enhancement. The interactive effect is not only an overlay of the influences of two factors but also an overlay of the influences of complex groups. For example, the groups of precipitation and temperature exhibit different enhancement patterns in North America and South America. This phenomenon could be attributed to the notable differences in climate and underlying surface conditions, which affect the patterns of SOC storage or release.

In general, temperature and precipitation are the main climate drivers, and the LAI is the crucial local factor. However, the positive or negative effects of these drivers on SOC sinks remain uncertain, which more notably depends on local conditions and the joint effect of multiple factors. A temperature increase in cold regions could cause frozen soil thawing and activate soil respiration, leading to SOC release. However, it could simultaneously stimulate vegetation emergence and even recovery, which contributes to SOC storage. If the inherent soil reserves are large, vegetation growth may lead to decomposition at relatively high temperatures. Temperature increases and precipitation variations could modulate vegetation cover conditions and even result in other related human land uses, such as farming. Moreover, wind and runoff play key roles in vegetation growth and SOC migration.

3.3. Accumulation and migration routes of global SOC storage

Based on the trend identification results shown in Fig. 1, we determined the main loss and accumulation areas of the global SOC stocks from obviously decreasing and increasing areas, respectively, considering regional proximity (Fig. S7 in Appendix A). The SOC reserves in regions with different latitudes, topographies and land use types are highly diverse under global warming. High-latitude and snow-covered areas are vulnerable to wind and freeze-thaw erosion processes, while more carbon is released, and these areas generally serve as a source of glacial and frozen soil degradation. The high-latitude permafrost above 60 degrees north latitude shown in Fig. S7 may be the main source of SOC loss. In low-latitude areas, the cultivated land area could serve as both a source and a sink. Plant and harvest processes disturb the soil conditions. Microorganism respiration becomes active, and carbon is released. Nevertheless, exposed soil is likely to take in CO_2 in the air as well as crop growth. Crop rotation promotes the growth of soil communities and enhances biological abiotic interactions, leading to a positive impact on the formation and storage of soil organic matter. Although the effect of carbon sinks is reduced after the conversion into arable land compared with that of forest land [45], it could be enhanced via reclamation and farmland management. Moreover, large amounts of residual plant matter after harvesting could increase the carbon reserves. SOC is generated from vegetation growth and sequestered from litter in the soil.

Nevertheless, water erosion provides a force for the leaching and movement of SOC in terms of precipitation and runoff. Thus, rivers carry SOC with low and sediment from upstream to downstream areas. There is an assumption regarding the geographical correlation whereby the increase in the lower reaches originates from the decrease in the upper reaches. In large river basins such as the Yangtze River Basin, the Mississippi River Basin, and the Congo River Basin, SOC obviously migrates with water flow and gradually accumulates downstream (Fig. S7). SOC generally flows from the upper reaches to the middle and lower reaches of rivers, and settles to stimulate vegetation growth for generating new SOC, or discharge into the sea. This movement occurs from high to low latitudes in the Northern Hemisphere. The SOC reserves decrease in high-latitude areas and increase in mid- and low-latitude areas. The main accumulation areas are mid- and low-latitude cultivated land and forestland areas, while the main loss areas are forestland, grassland, and frozen soil areas in high-latitude regions, as well as wasteland and plateau areas in mid- and low-latitude regions.

In the future, with the continuous climate change and global temperature rise, the impacts of wind and water erosion processes will intensify in high-latitude areas and plateau areas with less vegetation coverage. This will further reduce carbon storage in land surface soil in this area. At middle and low latitudes, under the implementation of conservation tillage measures and forestland protection policies, organic carbon storage in land surface soil may increase. In grassland and shrubland areas, the vegetation density and biological species may change under global warming, affecting the regional SOC storage and distribution.

3.4. Projection of global land surface SOC under future climate change

Future projections were obtained via 11 climate models under the SSP1-2.6, SSP2-4.5, SSP3-7.0, and SSP5-8.5 scenarios. The quantile correction method was employed to correct the CMIP6 precipitation and temperature data. The simulation data used are the average data of the individual corrected models, thereby reducing uncertainty. The global SOC generally increased under the different

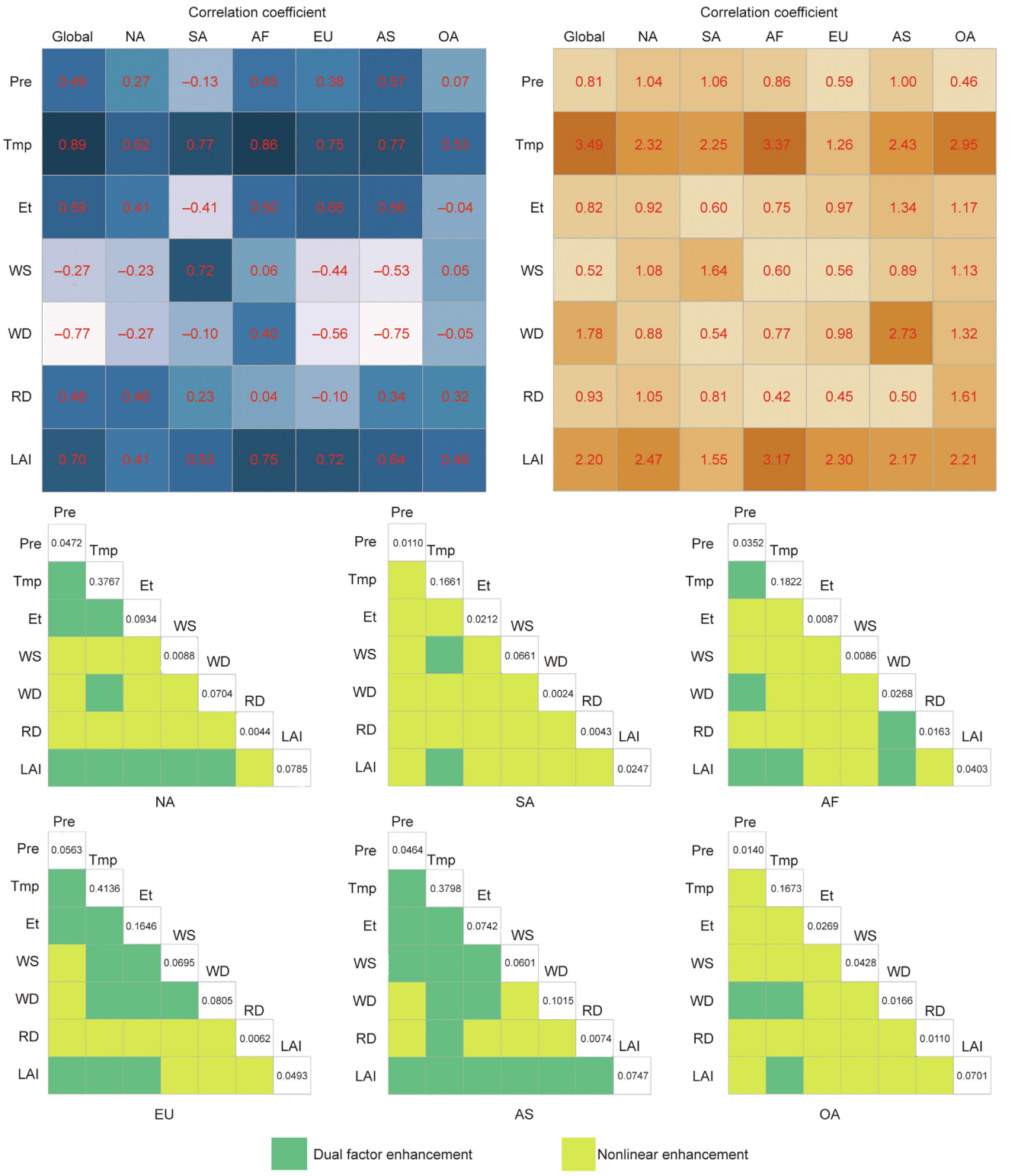

Fig.3. Correlation, importance, and interaction of the potential factors of precipitation (Pre), temperature (Tmp), evaporation (Et), wind speed (WS), rainfall days (WD), average runoff depth (RD), and LAI for global and continental SOC changes. The importance coefficients are obtained via the RF model and the interactive effects are calculated via the geographical detector model.

scenarios in the future (Fig. 4(a)). The high-emission scenarios indicated notable SOC growth. Africa and South America exhibited remarkable increasing trends, whereas North America, Asia, Europe, and Oceania exhibited contradictory trends.

Under SSP1-2.6, the global SOC average slightly increased by 4.34×10^{-4} t·ha^{-1} and basically remained stable until 2100, and the increasing trend was consistent across the different continents. Under SSP2-4.5, this global SOC average showed a similar increase as that under SSP1-2.6. However, it exhibited a greater variation of 0.254 t·ha^{-1}. This result demonstrated a significant average increase of 2.74×10^{-3} t·ha^{-1} and a variation of 0.4 t·ha^{-1} under SSP3-7.0 since this scenario represents moderate to high land use

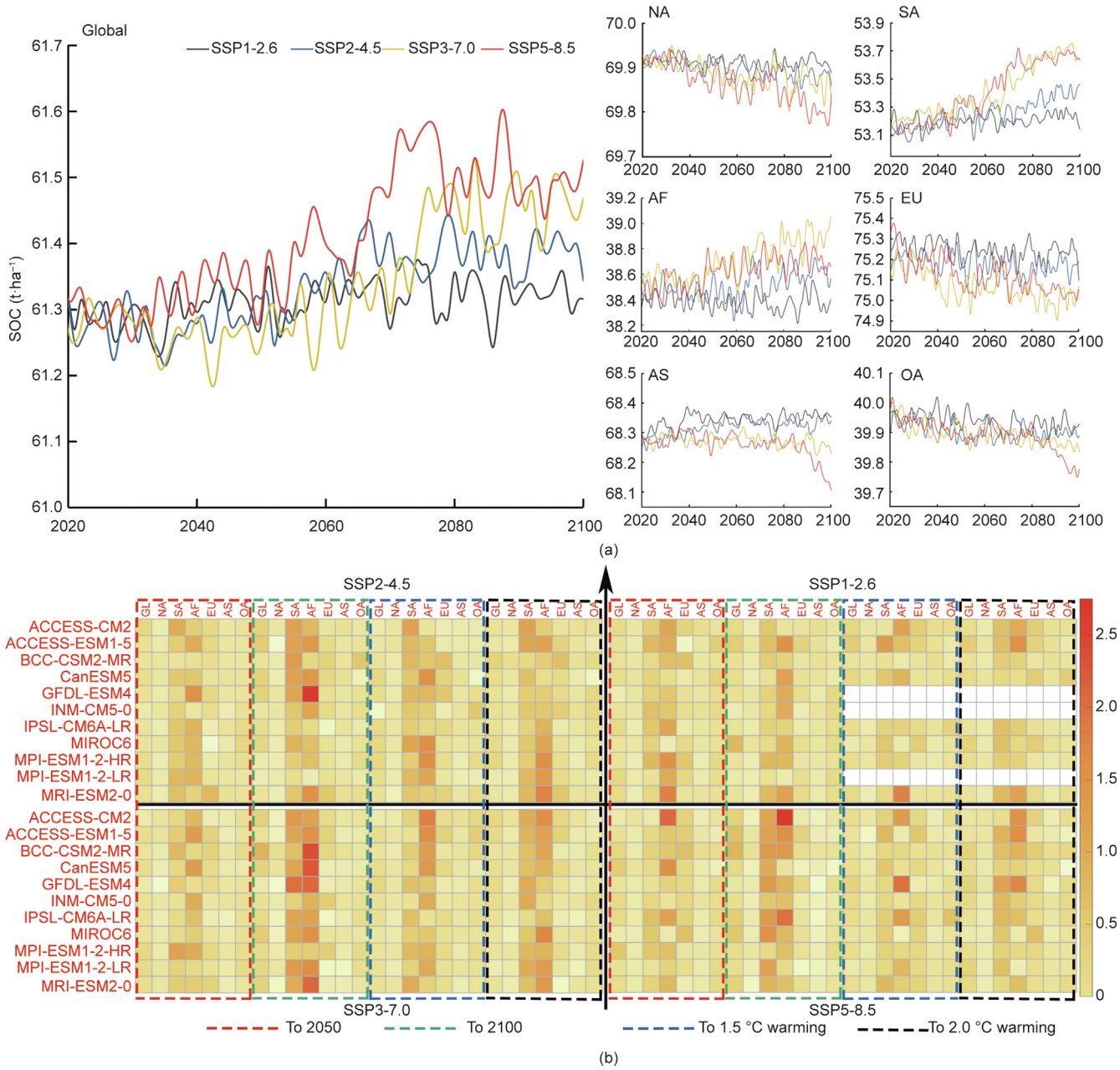

Fig. 4. Global and continental SOC change trends under the SSP1-2.6, SSP2-4.5, SSP3-7.0, and SSP5-8.5 scenarios with 11 global climate models of ACCESS-CM2, ACCESS-ESM1-5, BCC-CSM2-MR, CanESM5, GFDL-ESM4, INM-CM5-0, IPSL-CM6A-LR, MIROC6, MPI-ESM1-2-HR, MPI-ESM1-2-LR, and MRI-ESM2-0. (a) Average SOC change during the future period, (b) SOC change as the difference between the average SOC from 1981 to 2019 and that during the four future periods of 2050, 2100, 1.5 °C global warming, and 2.0 °C global warming scenarios. GL: global.

changes under high climate forcing. With respect to continents, the SOC stock in Africa and South America exhibited a notable increase, which probably occurred because the SOC stock in these continents is dominated by land cover. SSP5-8.5 showed drastic SOC changes, with an average increase of 3.25×10^{-3} t·ha^{-1} and a variation of 0.369 t·ha^{-1} due to the highest radiative forcing. Africa and South America are still major growth areas. Notably, North America, Asia, and Oceania demonstrated remarkable declines in the far future, which could probably be attributed to long-term high temperatures promoting SOC release and reducing sequestration.

In general, high-latitude zones, especially the northern latitudes of North America, Asia, and Europe, are the main areas with reduced SOC stocks, whereas the middle and low latitudes of Africa and South America are the primary reserve areas. The global variation in SOC could lead to risks. The significant increase in SOC storage in Africa and South America might affect ecosystem functioning and cause increased water consumption. Moreover, in loss areas, other forms of carbon, such as inorganic carbon, might accelerate the release process originally limited by SOC in the soil.

Furthermore, we explored the SOC change trends during four crucial periods, namely, 2050 (near future), 2100 (far future), and under global warming scenarios of 1.5 and 2 °C above preindustrial levels, under the four pathways, as shown in Fig. 4(b). The 1.5 °C global warming occurs from 2040 to 2045 according to the median values of the four pathways, while the 2 °C global warming occurs from 2047 to 2057. The different time nodes of global warming are

tied to sensitivity discrepancies to changes in atmospheric carbon dioxide, the physical representation of clouds, and responses of extratropical low cloud and water content to unforced variations in surface temperature [46].

Notably, South America and Africa exhibited significant SOC increases during all four periods under the four pathways. The SSP1-2.6 scenario exhibited the smallest change in SOC, and the simulations of three GCMs did not reach the 1.5 °C global warming level, whereas those of six GCMs did not reach the 2.0 °C global warming level until 2100. South America and Africa showed a very slight increase in SOC, with a value of 1.0 $t{\cdot}ha^{-1}$. Under SSP2-4.5, there was a relatively obvious increase until 2100, especially in South America and Africa, with a maximum increase of 2.0 $t{\cdot}ha^{-1}$. SOC increased significantly under the SSP3-7.0 and SSP5-8.5 scenarios, and SSP3-7.0 indicated a greater increase until 2100 since this scenario incorporates large land use changes. Since the SSP5-8.5 simulations reached the 1.5 and 2.0 °C global warming levels earlier, the SOC changes during these periods were not as notable as those under the other scenarios. However, the SOC increase under SSP5-8.5 was not necessarily greater than that under SSP3-7.0, although it accounts for higher emissions and stronger radiative forcing. SOC is positively associated with radiative forcing and global warming, but apparently, SOC change takes a little time due to lag feedback.

Spatial change could reflect the transformation of carbon sources and carbon sinks at the regional scale. Fig. S8 in Appendix A shows the spatial changes in SOC during the different periods under the four pathways. The global SOC stock basically increased over time under the 1.5 °C global warming, 2050, 2.0 °C global warming, and 2100 scenarios. Under the SSP1-2.6 and SSP2-4.5 scenarios, South America and Africa served as carbon sinks, which continued to increase. Under the SSP3-7.0 and SSP5-8.5 scenarios, these two continents more likely served as carbon sources before 2100. The increasing regions were located mainly at mid- and low-latitudes, and this trend extended to high-latitude regions over time until 2100. Until 2100, the differences in pathways clearly decreased, and SOC increased worldwide. The spatial change distributions clearly indicated that SOC storage did not increase from SSP3-7.0 (17.259 PgC) to SSP5-8.5 (16.944 PgC) in 2100, although the radiative forcing obviously increased. This could occur because SOC changes also depend on the underlying surface, such as land cover. Moreover, due to the advancement of the occurrence of temperature increase, the change under the SSP3-7.0 and SSP5-8.5 scenarios were not as remarkable as those under the SSP1-2.6 and SSP2-4.5 scenarios at the time nodes of 1.5 and 2.0 °C global warming. Overall, large river basins located at mid- and low-latitudes were typical regions where SOC increased, whereas high-latitude areas affected by relatively high temperatures and wind speeds became SOC loss regions. With accumulation over time and increasing temperatures, this change could increase notably.

4. Discussion

Since the 1990s, global warming has caused an increase in the land surface SOC stock below 0.3 m. Over the last 39 years, from 1981 to 2019, the global land surface SOC stock increased by 6.393 PgC. This trend conformed with the increase in the global forest carbon sink [47], and the terrestrial carbon sink increased from (-0.2 ± 0.9) $PgC{\cdot}a^{-1}$ in 1960 to (1.9 ± 1.1) $PgC{\cdot}a^{-1}$ in 2010 [48]. Piao et al. [49] also reported that the terrestrial carbon sink increased from 1998 to 2012, and the linear trend of the net land carbon sink was (0.17 ± 0.05) $PgC{\cdot}a^{-2}$, which is three times greater than that from 1980 to 1998 ((0.05 ± 0.05) $PgC{\cdot}a^{-2}$). Temperature, precipitation, and vegetation cover (LAI) are the main drivers, while the temperature and LAI generally yield dual factor enhancements with other factors on the different continents. The factors of precipitation, temperature, evaporation, wind speed, rainfall days, average runoff depth, and LAI generate varying effects on the different continents. These climate and underlying surface factors provide an enhancement and synergy for global and continental SOC variations. Climate plays a key role in regulating plant growth and potential carbon storage in soil.

Vegetation determines the net carbon input into the soil system and the quality and vulnerability of soil organic matter, while dense vegetation cover exhibits a relatively high SOC density [50]. The increase in vegetation cover accounts for most of the increase in the global SOC stock. With increasing temperature and precipitation, the vegetation cover at lower latitudes increases, and vegetation emerges in the tundra in high-altitude cold regions. In 2016, tree coverage increased by 7.1% relative to the 1982 level [51], and the increase in the LAI alone was responsible for 12.4% of the total terrestrial carbon sink ((95 ± 5) PgC) from 1981 to 2016 [18]. Vegetation can generate new SOC, and SOC, as the most important indicator of soil fertility and productivity, stimulates vegetation growth. The virtuous cycle could accelerate SOC sequestration, especially in downstream and plain terrains in mid- and low-latitude regions.

The global SOC stock in the future will increase compared with the average SOC stock from 1981 to 2019 according to CMIP6 predictions under the SSP1-2.6, SSP2-4.5, SSP3-7.0, and SSP5-8.5 scenarios. By 2100, the increase in the global SOC stock will increase by 13.0–17.2 PgC. Notably, the future SOC variation projection does not include the effects of land use and management measures related to climate change. These results agree with the overall increase in the global SOC stocks in the 21st century according to process-based vegetation carbon models under climate change [30,52]. Global terrestrial carbon sinks would increase by 0.9–3.3 $PgC{\cdot}a^{-1}$ [53,54], whereas a more conservative estimate is an increase ranging from 0.3 to 0.7 $PgC{\cdot}a^{-1}$ [55]. Ito et al. [56] employed earth system models and predicted that the total SOC stock increased over the historical period ((30 ± 67) PgC) (1850–2014) and under future (2015–2100) climate and land conditions ((48 ± 32) PgC for SSP1-2.6 and (49 ± 58) PgC for SSP3-7.0), and they indicated that the total SOC content will increase at a modest rate of approximately 0.04% per year (0.6 $PgC{\cdot}a^{-1}$). The increase in the future global SOC stock is certain, although the exact increase varies due to the different benchmarks used for comparison, simulation models, and data.

The Paris Agreement aims to maintain the global average temperature increase to well below 2 °C above preindustrial levels and even aims to limit the increase to less than 1.5 °C. However, from 2013 to 2022, greenhouse gas emissions reached an overall high level of (54 ± 5.3) gigatonnes of carbon dioxide ($GtCO_2$) over the last decade, and human-induced warming has increased at an unprecedented rate of more than 0.2 °C per year [57]. According to the estimates from the Sixth Assessment Report (AR6) of Working Group I (WGI) and Working Group III (WGIII), the remaining carbon budget for the 1.5 °C global warming target decreased from 500 $GtCO_2$ in 2020 to 250 $GtCO_2$ in 2023, with a warming update (2013–2022). Under the 1.5 °C climate warming target, the land SOC sink will increase by approximately 13.0 PgC (47.6 $GtCO_2$) at most from that under SSP1-2.6, which accounts for only 19.0% of the total carbon emission capacity at the current 1.1 to 1.5 °C global warming level. Even our most optimistic estimate of a maximum increase of 17.2 PgC (63.0 $GtCO_2$) until 2100 compared with the historical average represents only a quarter of the contribution to CO_2 intake from the soil. Natural land-based mitigation is very limited, and the Paris Agreement target of a four out of one thousand increase in soil carbon stocks 40 cm below the surface per year over the next 20 years is ambitious (2.72 $PgC{\cdot}a^{-1}$, a four

out of one thousand of 0.68 trillion tonnes of the land surface SOC stock at 30 cm below the surface).

However, the predictions of future SOC changes vary with a climate model, emission scenario, and study region. Yigini and Panagos [24] employed a geostatistical model to predict an overall increase in SOC stocks by 2050 in Europe for all climate scenarios under CMIP5. Olaya-Abril et al. [58] reported that the SOC concentration in southern Spain may decline by 35.4% under a high-emission scenario. Gautam et al. [33] reported that machine learning approach estimates revealed a mean total loss of 1.8 PgC in US surface soils under a high-emission scenario by 2100, whereas earth system models revealed no significant change in SOC stocks, with wide variation among these models. Walker et al. [59] projected that the potential for additional carbon storage in woody biomass will increase (17%) by 2050 despite projected decreases (−12%) in the tropics. Wang et al. [60] applied an innovative approach that combines space-for-time substitution with meta-analysis and reported that the SOC stock will decrease by 6.0% ± 1.6% at the 0–0.3 m soil depth under 1 °C warming. The warming group generation process (cropland excluded) and steady-state assumption for the actual carbon stock introduced additional uncertainty. The differences in the simulated changes in SOC stocks among various studies are related to the complex interrelationships between the factors that determine the C balance of soils in biophysical models and uncertainties in future climate projections [31].

The prediction of soil carbon climate feedback is highly uncertain as a result of different model structures, parameter values, and initial conditions. Models predicted a wider range of future soil carbon changes and diverse trajectories with both negative and positive feedback [61]. On the one hand, a complete process-based understanding remains lacking due to the complexities of the drivers of SOC. Whether current models are suitable representations of the mechanisms of soil carbon dynamics remains uncertain. On the other hand, more observations are needed to better constrain the model parameters. The need for data processing is another limitation, as data are collected on a small spatial scale and cannot provide suitable global parameter constraints because of the lack of an effective upscaling scheme. The widely used steady-state assumption yields a mismatch in the actual carbon stock. In addition, inorganic carbon in terms of carbonates, bicarbonates, and coal particles could occur in soil along with organic carbon, which affects the calculation of the total SOC stock. Although its contribution is very limited at the global scale, the influence of inorganic carbon cannot be ignored and should be addressed in SOC studies, such as regional or single-site studies.

In numerous studies, machine learning methods have been applied, which have been verified as accurate and effective in estimating and mapping SOC stocks [62]. We adopted the widely used RF model, fully examined the feedback of SOC to environmental conditions, and projected the future SOC stock based on the historical link embodied in the model. Compared with the microbial model and experimental methods, this method could better reflect the inherent mechanism and the correlation between initial conditions and projected soil carbon from large-scale time-series data. Additionally, we employed a reconstructed dataset [36,37] based on global SOC measurements (SOC-1 km), which overcomes the issues of uneven spatial distributions and heterogeneity in data obtained from direct observation stations. The long-term series of SOC stocks were estimated via a digital soil mapping model and the RothC-simulated method, thereby incorporating climate, landform, soil, and land use types. The dataset processing step included the potential drivers of SOC. The SOC-1km dataset demonstrated better performance than that of the WoSIS, SoilGrids, and HWSD SOC datasets, as described in Text S5 in Appendix A. Thus, it is reasonable to expect that our global SOC variation and projection results exhibit a certain degree of credibility, which also conforms with the increase in the historical SOC variation under global greening and warming. Notably, the proposed RF model did not account for changes in land use and management. One reason is that this study focused on natural global surface SOC changes to support the formulation of soil and land management strategies for soil carbon sequestration programs. In addition, future land use and management are more uncertain since they are likely to be adjusted according to the policies associated with social and economic development goals. These variable conditions cannot be fully incorporated into the RF model as a learning rule, which results in error. The full consideration of natural and human-induced factors calls for a complete process-based model in the future.

There are several limitations to this method, but the main drivers of dynamic factors are captured. Factors other than precipitation and the daily temperature, such as elevated CO_2 levels, nitrogen deposition, fires, and extreme weather events, could affect SOC variation. Elevated CO_2 levels may stimulate plant growth and alter carbon inputs into the soil. Our results might overestimate the global SOC increase considering the negative effects of nitrogen deposition, especially in boreal cold regions, and the additional release resulting from the occurrence of extreme weather events. Warming can cause more severe and frequent fires, extreme weather, and even flood and drought disasters. Fires may directly change the local soil carbon status in terms of both quantity and quality (e.g., greater pyrogenic carbon inputs) and the physicochemical environment for SOC decomposition [63]. Extreme precipitation and floods can lead to soil erosion and drive SOC movement. Extreme daily temperatures and drought can cause vegetation to wither and degrade. These factors may also interact with warming to determine the net balance of SOC under warming. Although we implicitly included these effects in the vegetation index, the role of soil intake and output-induced factors should be further elucidated for a more accurate estimation of the global SOC stock.

An accurate SOC projection relies on detailed data from a comprehensive monitoring system. Glacial permafrost soil contains a considerable amount of SOC, dissolved organic carbon, or other forms of carbon. As permafrost melts, dissolved organic carbon is released via microbial decomposition or even due to wind erosion, and new SOC is generated if new vegetation is present. Forest, grassland, and cropland ecosystems should also be key monitoring areas as their carbon pools notably affect SOC changes. Moreover, extreme weather events caused by precipitation should be considered, since flooding could lead to more erosion-related SOC release. Extreme temperature events can cause fires and modulate SOC conditions. Human activities related to land use change synergistically affect SOC stocks. As a promising natural solution for carbon sinks, soil effects should be monitored and assessed objectively to implement timely, effective measures for more time-efficient maintenance of the global carbon equilibrium.

5. Conclusions

Since the “4 per 1000” Initiative of a four out of one thousand increase in the soil carbon stocks 40 cm below the surface per year over the next 20 years was proposed by the French government at the Conference of the Parties 22 (COP21) Paris climate summit in 2015, natural land-based mitigation has attracted increased attention with the aim to reach the target of global carbon equilibrium. The “4 per 1000” Initiative promotes soil carbon sequestration via appropriate land and soil management. It has been recognized that the global carbon soil stock will increase under global greening and warming, but the mechanism and quantity remain unknown.

Understanding how it will change under global warming in a natural manner is crucial for more effective decision-making regarding land and soil management measures and even for formulating carbon mitigation and removal strategies.

In this paper, the mechanism of global land surface SOC evolution and its driving factors were identified, and an RF model integrating the inherent mechanism from large-scale long time-series data was proposed. The future trends in global surface soil stocks were quantitatively projected. The results revealed that the global surface SOC increase driven by climate change is far from the Paris Agreement target of a four out of one thousand increase in the soil carbon stocks 40 cm below the surface per year over the next 20 years, which illustrates that the "4 per 1000" Initiative more notably depends on effective human-induced measures. Over-reliance on natural carbon sinks is a risky strategy. These findings highlight the urgency of implementing mitigation and removal strategies to reduce greenhouse gas emissions, which is consistent with the topic of Conference of the Parties 28 (COP28) but is very time-sensitive. The ambitious mitigation scenarios require even greater land area or additional land-use changes, such as biomass energy with capture and storage strategies for CO_2 removal. The global carbon equilibrium, or the Paris Agreement target, is more likely to rely on mitigation and removal strategies for greenhouse emissions. Enormous investments and advanced technology for limiting emissions, combined with carbon capture and storage, could possibly reverse the warming trend, but this depends on the feasibility on a large enough scale.

Despite the notable uncertainties in the machine learning method employed, it can capture the feedback of SOC to environmental conditions, better reflect the inherent mechanism and the correlation among initial conditions, and provide future projections without the steady-state assumption. Compared with the microbial model and experimental methods, which are limited to the regional scale, the proposed RF model provides a more effective way to explore SOC evolution patterns at the global and long-term scales. However, more reliable data from comprehensive monitoring systems and advanced data-processing techniques are needed for obtaining accurate projections and establishing effective carbon strategies, especially when considering a climate change tipping point nearing.

CRediT authorship contribution statement

Yanli Liu: Writing – review & editing, Writing – original draft, Conceptualization. **Xin Chen:** Formal analysis, Data curation. **Jianyun Zhang:** Supervision, Methodology, Formal analysis. **Xing Yuan:** Validation. **Tiesheng Guan:** Resources, Investigation. **Junliang Jin:** Software, Investigation. **Guoqing Wang:** Visualization, Methodology.

Declaration of competing interest

The authors declare that they have no known competing financial interests or personal relationships that could have appeared to influence the work reported in this paper.

Acknowledgments

This work was supported by the National Natural Science Foundation of China (52325902, 52361145889, 52121006, and U2240203). The authors acknowledge the data support received from the National Earth System Science Data Center, National Science and Technology Infrastructure of China. We thank the reviewers and the editor for their constructive comments.

Appendix A. Supplementary data

Supplementary data to this article can be found online at https://doi.org/10.1016/j.eng.2025.03.031.

References

[1] Smith P. Soils and climate change. Curr Opin Environ Sustain 2012;4(5):539–44.
[2] Jones C, Robertson E, Arora V, Friedlingstein P, Shevliakova E, Bopp L, et al. Twenty-first-century compatible CO_2 emissions and airborne fraction simulated by CMIP5 earth system models under four representative concentration pathways. J Clim 2013;26(13):4398–413.
[3] Bossio DA, Cook-Patton SC, Ellis PW, Fargione J, Sanderman J, Smith P, et al. The role of soil carbon in natural climate solutions. Nat Sustain 2020;3(5):391–8.
[4] Jenkinson DS, Adams DE, Wild A. Model estimates of CO_2 emissions from soil in response to global warming. Nature 1991;351(6324):304–6.
[5] Cox PM, Betts RA, Jones CD, Spall SA, Totterdell IJ. Acceleration of global warming due to carbon-cycle feedbacks in a coupled climate model. Nature 2000;408(6809):184–7.
[6] Bradford MA, Wieder WR, Bonan GB, Fierer N, Raymond PA, Crowther TW. Managing uncertainty in soil carbon feedbacks to climate change. Nat Clim Chang 2016;6(8):751–8.
[7] Todd-Brown KEO, Randerson JT, Hopkins F, Arora V, Hajima T, Jones C, et al. Changes in soil organic carbon storage predicted by Earth system models during the 21st century. Biogeosciences 2014;11(8):2341–56.
[8] O'sullivan M, Friedlingstein P, Sitch S, Anthoni P, Arneth A, Arora VK, et al. Process-oriented analysis of dominant sources of uncertainty in the land carbon sink. Nat Commun 2022;13(1):4781.
[9] Arrouays D, Deslais W, Badeau V. The carbon content of topsoil and its geographical distribution in France. Soil Use Manage 2001;17(1):7–11.
[10] Jia X, Li X, Zhang Z. Spatial heterogeneity of soil organic carbon and nitrogen under Ammopiptanhus mongolicus community in arid desert zone. Chin J Appl Ecol 2006;17(12):2266–70. Chinese.
[11] Kolby Smith W, Reed SC, Cleveland CC, Ballantyne AP, Anderegg WRL, Wieder WR, et al. Large divergence of satellite and Earth system model estimates of global terrestrial CO_2 fertilization. Nat Clim Chang 2016;6(3):306–10.
[12] Soleimani A, Hosseini SM, Bavani ARM, Jafari M, Francaviglia R. Simulating soil organic carbon stock as affected by land cover change and climate change, Hyrcanian forests (northern Iran). Sci Total Environ 2017;599–600:1646–57.
[13] Bennett LT, Hinko-Najera N, Aponte C, Nitschke CR, Fairman TA, Fedrigo M, et al. Refining benchmarks for soil organic carbon in Australia's temperate forests. Geoderma 2020;368:114246.
[14] Gottschalk P, Smith JU, Wattenbach M, Bellarby J, Stehfest E, Arnell N, et al. How will organic carbon stocks in mineral soils evolve under future climate? Global projections using RothC for a range of climate change scenarios. Biogeosciences 2012;9(8):3151–71.
[15] Lucht W, Schaphoff S, Erbrecht T, Heyder U, Cramer W. Terrestrial vegetation redistribution and carbon balance under climate change. Carbon Balance Manag 2006;1:1–7.
[16] Arora VK, Boer GJ, Friedlingstein P, Eby M, Jones CD, Christian JR, et al. Carbon–concentration and carbon–climate feedbacks in CMIP5 Earth system models. J Clim 2013;26(15):5289–314.
[17] Quinn Thomas R, Canham CD, Weathers KC, Goodale CL. Increased tree carbon storage in response to nitrogen deposition in the US. Nat Geosci 2010;3(1):13–7.
[18] Chen JM, Ju W, Ciais P, Viovy N, Liu R, Liu Y. Vegetation structural change since 1981 significantly enhanced the terrestrial carbon sink. Nat Commun 2019;10(1):4259.
[19] Fu C, Li Y, Zeng L, Zhang H, Tu C, Zhou Q, et al. Stocks and losses of soil organic carbon from Chinese vegetated coastal habitats. Glob Change Biol 2021;27(1):202–14.
[20] Lu X, Vitousek PM, Mao Q, Gilliam FS, Luo Y, Turner BL, et al. Nitrogen deposition accelerates soil carbon sequestration in tropical forests. Proc Natl Acad Sci USA 2021;118(16):e2020790118.
[21] Yamashita N, Ishizuka S, Hashimoto S, Ugawa S, Nanko K, Osone Y, et al. National-scale 3D mapping of soil organic carbon in a Japanese forest considering microtopography and tephra deposition. Geoderma 2022;406:115534.
[22] Liang J, Chen K, Siqintana HT, Zhang Y, Jing J, Feng W, et al. Towards improved modeling of SOC decomposition: soil water potential beyond the wilting point. Glob Change Biol 2022;28(11):3665–73.
[23] Lozano-García B, Muñoz-Rojas M, Parras-Alcántara L. Climate and land use changes effects on soil organic carbon stocks in a Mediterranean semi-natural area. Sci Total Environ 2017;579:1249–59.
[24] Yigini Y, Panagos P. Assessment of soil organic carbon stocks under future climate and land cover changes in Europe. Sci Total Environ 2016;557:838–50.
[25] Commonwealth Scientific and Industrial Research Organization (CSIRO) and Australian Bureau of Meteorology. Climate change in Australia information for Australia's natural resource management regions: technical report. Report. Canberra: CSIRO; 2015.
[26] Knutti R. The end of model democracy? An editorial comment. Clim Change 2010;102(3):395–404.

[27] Lobell DB, Hammer GL, Chenu K, Zheng B, McLean G, Chapman SC, et al. The shifting influence of drought and heat stress for crops in northeast Australia. Glob Change Biol 2015;21(11):4115–27.
[28] Ukkola AM, De Kauwe MG, Roderick ML, Abramowitz G, Pitman AJ. Robust future changes in meteorological drought in CMIP6 projections despite uncertainty in precipitation. Geophys Res Lett 2020;47(11):e2020GL087820.
[29] Cannon AJ. Reductions in daily continental-scale atmospheric circulation biases between generations of global climate models: CMIP5 to CMIP6. Environ Res Lett 2020;15(6):064006.
[30] Adhikari K, Owens PR, Libohova Z, Miller DM, Wills SA, Nemecek J. Assessing soil organic carbon stock of Wisconsin, USA and its fate under future land use and climate change. Sci Total Environ 2019;667:833–45.
[31] Wang B, Gray JM, Waters CM, Anwar MR, Orgill SE, Cowie AL. Modelling and mapping soil organic carbon stocks under future climate change in south–eastern Australia. Geoderma 2022;405:115442.
[32] Kunkel VR, Wells T, Hancock GR. Modelling soil organic carbon using vegetation indices across large catchments in eastern Australia. Sci Total Environ 2022;817:152690.
[33] Gautam S, Mishra U, Scown CD, Wills SA, Adhikari K, Drewniak BA. Continental United States may lose 1.8 petagrams of soil organic carbon under climate change by 2100. Glob Ecol Biogeogr 2022;31(5/6):1147–60.
[34] Gibson AJ, Hancock GR, Verdon-Kidd DC, Martinez C, Wells T. The impact of shifting Köppen-Geiger climate zones on soil organic carbon concentrations in Australian grasslands. Glob Planet Change 2021;202:103523.
[35] Jungkunst HF, Göpel J, Horvath T, Ott S, Brunn M. Global soil organic carbon–climate interactions: why scales matter. WIREs Clim Change 2022;13(4):e780.
[36] Xie E, Zhang X, Lu F, Peng Y, Chen J, Zhao Y, et al. Integration of a process-based model into the digital soil mapping improves the space–time soil organic carbon modelling in intensively human-impacted area. Geoderma 2022;409:115599.
[37] Zhao YC, Xie EZ, Zhang X, Peng Y. Global topsoil SOC stock from 1981 to 2018 estimated by combining process-based model and space-for-time digital soil mapping [Internet]. Genève: Zenodo; 2021 Jun 29 [cited 2025 Mar 20]. Available from: https://zenodo.org/records/5040380.
[38] Zhang L, Zheng Q, Liu Y, Liu S, Yu D, Shi X, et al. Combined effects of temperature and precipitation on soil organic carbon changes in the uplands of eastern China. Geoderma 2019;337:1105–15.
[39] Wang C, Wang S, Fu B, Li Z, Wu X, Tang Q. Precipitation gradient determines the tradeoff between soil moisture and soil organic carbon, total nitrogen, and species richness in the Loess Plateau, China. Sci Total Environ 2017;575:1538–45.
[40] Luo Z, Feng W, Luo Y, Baldock J, Wang E. Soil organic carbon dynamics jointly controlled by climate, carbon inputs, soil properties and soil carbon fractions. Glob Change Biol 2017;23(10):4430–9.
[41] Zhou Y, Hartemink AE, Shi Z, Liang Z, Lu Y. Land use and climate change effects on soil organic carbon in north and northeast China. Sci Total Environ 2019;647:1230–8.
[42] Chen X, Deng Q, Lin G, Lin M, Wei H. Changing rainfall frequency affects soil organic carbon concentrations by altering non-labile soil organic carbon concentrations in a tropical monsoon forest. Sci Total Environ 2018;644:762–9.
[43] Chappell A, Webb NP, Leys JF, Waters CM, Orgill S, Eyres MJ. Minimising soil organic carbon erosion by wind is critical for land degradation neutrality. Environ Sci Policy 2019;93:43–52.
[44] Chowaniak M, Głąb T, Klima K, Niemiec M, Zaleski T, Zuzek D. Effect of tillage and crop management on runoff, soil erosion and organic carbon loss. Soil Use Manage 2020;36(4):581–93.
[45] Yu Z, Ciais P, Piao S, Houghton RA, Lu C, Tian H, et al. Forest expansion dominates China's land carbon sink since 1980. Nat Commun 2022;13(1):5374.
[46] Zelinka MD, Myers TA, McCoy DT, Chedley SP, Caldwell PM, Ceppi P, et al. Causes of higher climate sensitivity in CMIP6 models. Geophys Res Lett 2020;47(1):e2019GL085782.
[47] Tagesson T, Schurgers G, Horion S, Ciais P, Tian F, Brandt M, et al. Recent divergence in the contributions of tropical and boreal forests to the terrestrial carbon sink. Nat Ecol Evol 2020;4(2):202–9.
[48] Ballantyne AP, Alden CB, Miller JB, Tans PP, White JWC. Increase in observed net carbon dioxide uptake by land and oceans during the past 50 years. Nature 2012;488(7409):70–2.
[49] Piao S, Huang M, Liu Z, Wang X, Ciais P, Canadell JG, et al. Lower land-use emissions responsible for increased net land carbon sink during the slow warming period. Nat Geosci 2018;11(10):739–43.
[50] Kumar P, Sajjad H, Tripathy BR, Ahmed R, Manda VP. Prediction of spatial soil organic carbon distribution using Sentinel-2A and field inventory data in Sariska Tiger Reserve. Nat Hazards 2018;90:693–704.
[51] Song XP, Hansen MC, Stehman SV, Potapov PV, Tyukavina A, Vermote EF, et al. Global land change from 1982 to 2016. Nature 2018;560(7720):639–43.
[52] Rial M, Cortizas AM, Taboada T, Rodríguez-Lado L. Soil organic carbon stocks in Santa Cruz Island, Galapagos, under different climate change scenarios. Catena 2017;156:74–81.
[53] Smith P, Adams J, Beerling DJ, Beringer T, Calvin KV, Fuss S, et al. Land-management options for greenhouse gas removal and their impacts on ecosystem services and the sustainable development goals. Annu Rev Environ Resour 2019;44:255–86.
[54] Griscom BW, Adams J, Ellis PW, Houghton RA, Lomax G, Miteva DA, et al. Natural climate solutions. Proc Natl Acad Sci USA 2017;114(44):11645–50.
[55] Nolan CJ, Field CB, Mach KJ. Constraints and enablers for increasing carbon storage in the terrestrial biosphere. Nat Rev Earth Environ 2021;2(6):436–46.
[56] Ito A, Hajima T, Lawrence DM, Brovkin V, Delire C, Guenet B, et al. Soil carbon sequestration simulated in CMIP6-LUMIP models: implications for climatic mitigation. Environ Res Lett 2020;15(12):124061.
[57] Forster PM, Smith CJ, Walsh T, Lamb WF, Lamboll R, Hauser M, et al. Indicators of Global Climate Change 2022: annual update of large-scale indicators of the state of the climate system and human influence. Earth Syst Sci Data 2023;15:2295–327.
[58] Olaya-Abril Alfonso, Parras-Alcantara Luis, Lozano-García Beatriz, Obregon-´Romero Rafael. Soil organic carbon distribution in Mediterranean areas under a climate change scenario via multiple linear regression analysis. Sci Total Environ 2017;592:134–43.
[59] Walker WS, Gorelik SR, Cook-Patton SC, Baccini A, Farina MK, Solvik KK, et al. The global potential for increased storage of carbon on land. Proc Natl Acad Sci USA 2022;119:e2111312119.
[60] Wang M, Guo X, Zhang S, Xiao L, Mishra U, Yang Y, et al. Global soil profiles indicate depth-dependent soil carbon losses under a warmer climate. Nat Commun 2022;13:5514.
[61] Shi Z, Crowell S, Luo Y, Moore III B. Model structures amplify uncertainty in predicted soil carbon responses to climate change. Nat Commun 2018;9:2171.
[62] José P, Minasny B, Mcbratney AB. Machine learning and soil sciences: a review aided by machine learning tools. Soil 2020;6(1):35–52.
[63] Pellegrini AFA, Harden J, Georgiou K, Hemes KS, Malhotra A, Nolan CJ. Fire effects on the persistence of soil organic matter and long-term carbon storage. Nat Geosci 2021;15:5–13.